

**Overview of The 180° Ambiguity in
Solar Vector Magnetic Field Measurements
(especially for HMI)
and Present Methods for Solving It
(especially for HMI)**

K. D. Leka

with

Graham Barnes

Ashley Crouch

CoRA division

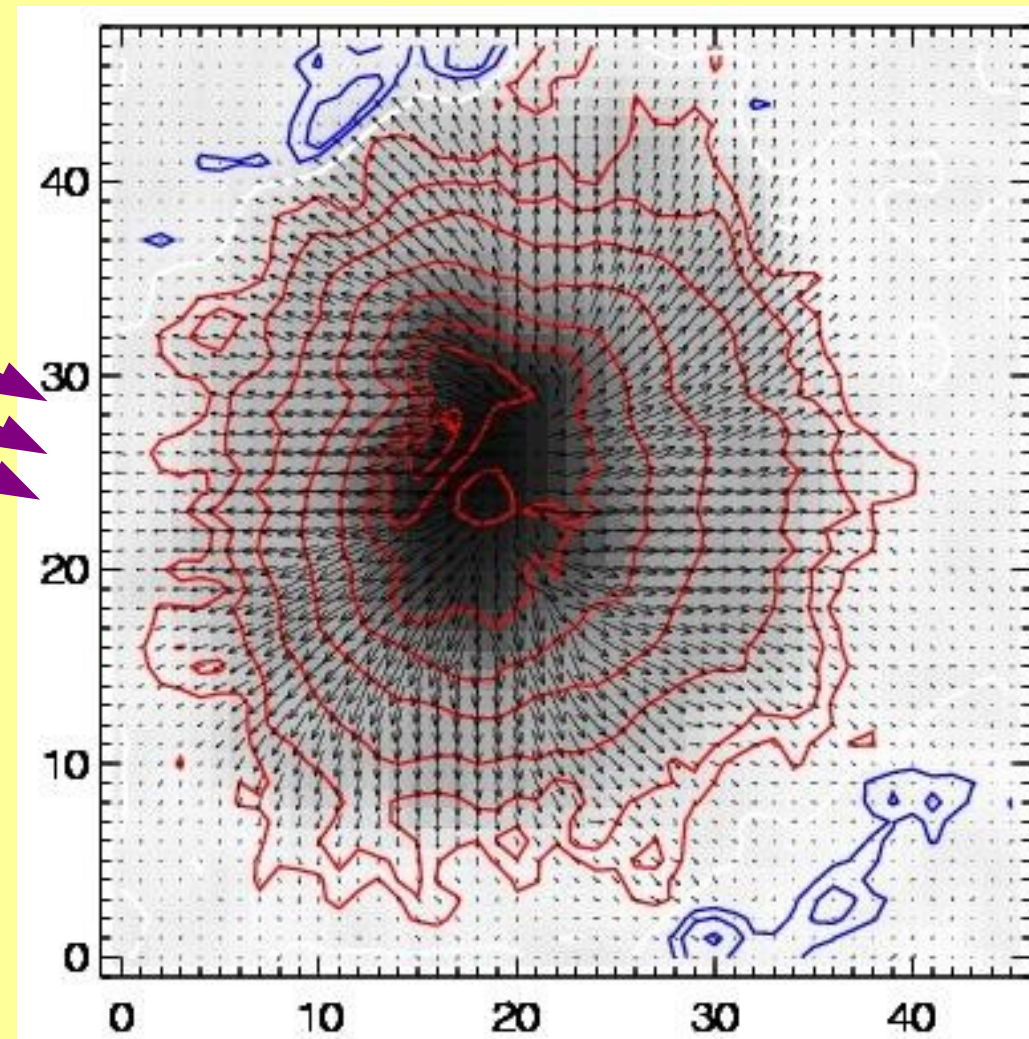
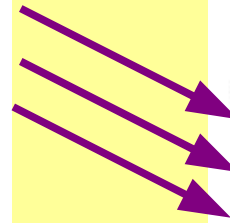
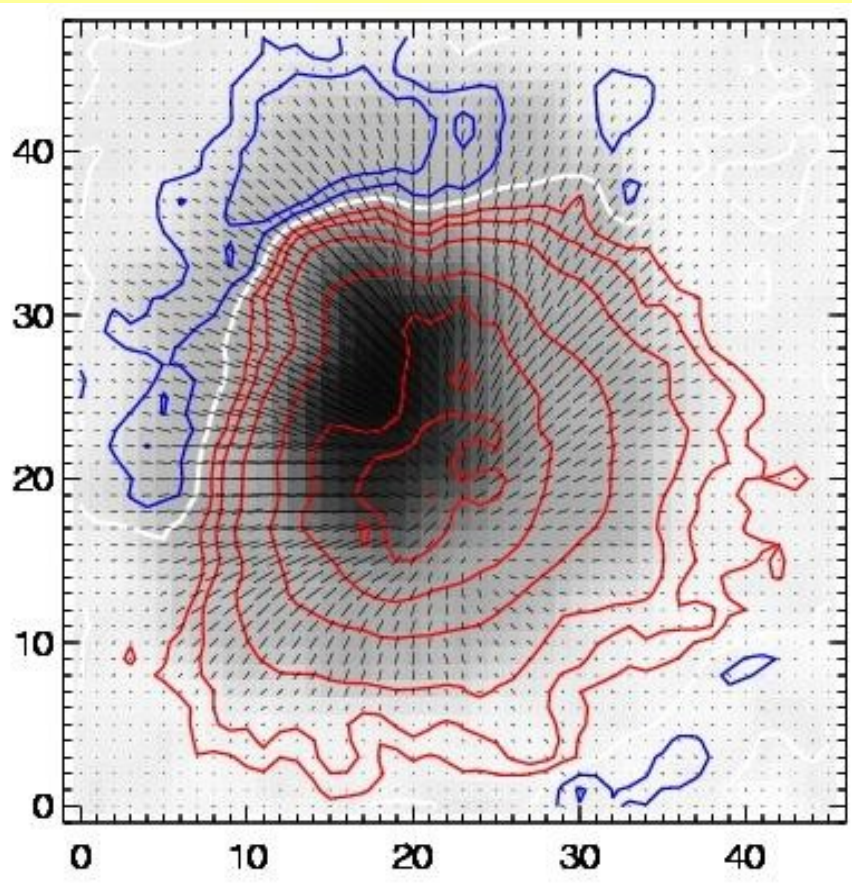
NorthWest Research Associates

Boulder, Colorado

- *Observations are only physical* after ambiguity resolution and expressed as heliographic ***B***

Red/Blue: line-of-sight flux B_{\parallel}
White: apparent polarity inversion
line, Line-segments: B_{\perp} magnitude
& direction. Sunspot is NE at $\mu \approx 0.8$.

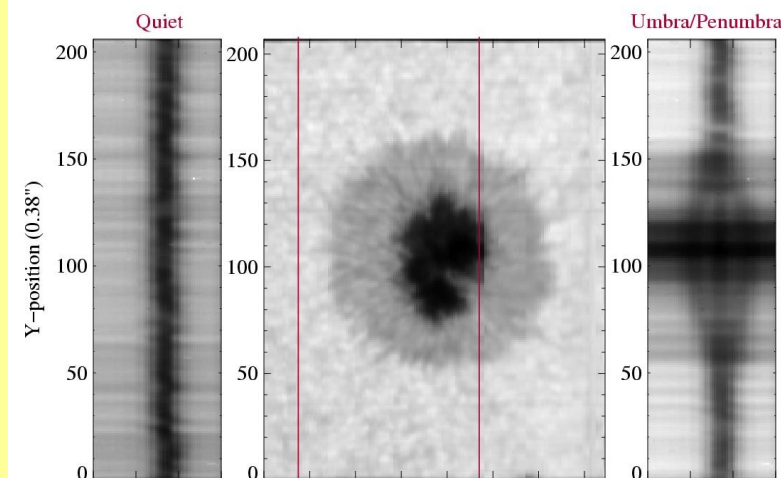
Heliographic *B*, azimuth resolved
(note shift in neutral line)



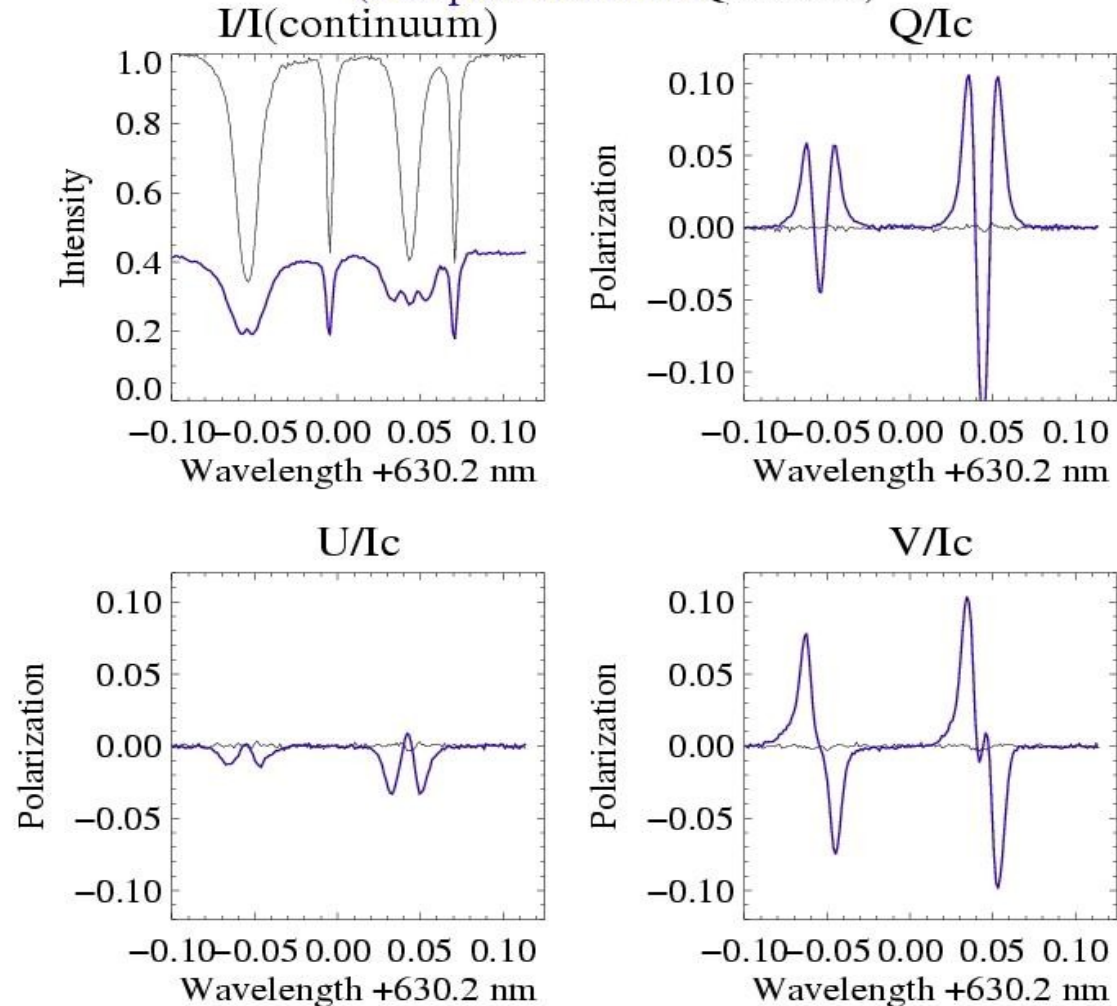
Intro to measuring photospheric magnetic field:

Stokes spectropolarimetry:

- Zeeman effect: magnetic field induces both energy-level splitting and polarization to emergent light of magnetically sensitive lines.
- Splitting proportional to $|\mathbf{B}|$:
- Split components are polarized:
 - For B_{\perp} : π components are polarized parallel to B_{\perp} , σ components are polarized perpendicular to B_{\perp}
 - For B_{\parallel} : π components are not visible, and σ components are circularly polarized.
- Final shape of polarization spectra and degree of polarization due to: strength, direction of magnetic field, thermodynamics of plasma, spatial and spectral resolution.
 - Quick reference:
 - $B_{\parallel} \propto V$
 - $B_{\perp} \propto (Q^2 + U^2)^{1/2}$
 - $\Phi \approx \tan^{-1}(U/Q) \rightarrow -90^{\circ} < \Phi < 90^{\circ}$




Stokes Polarization Signals
(Sunspot Penumbra/ Quiet Sun)

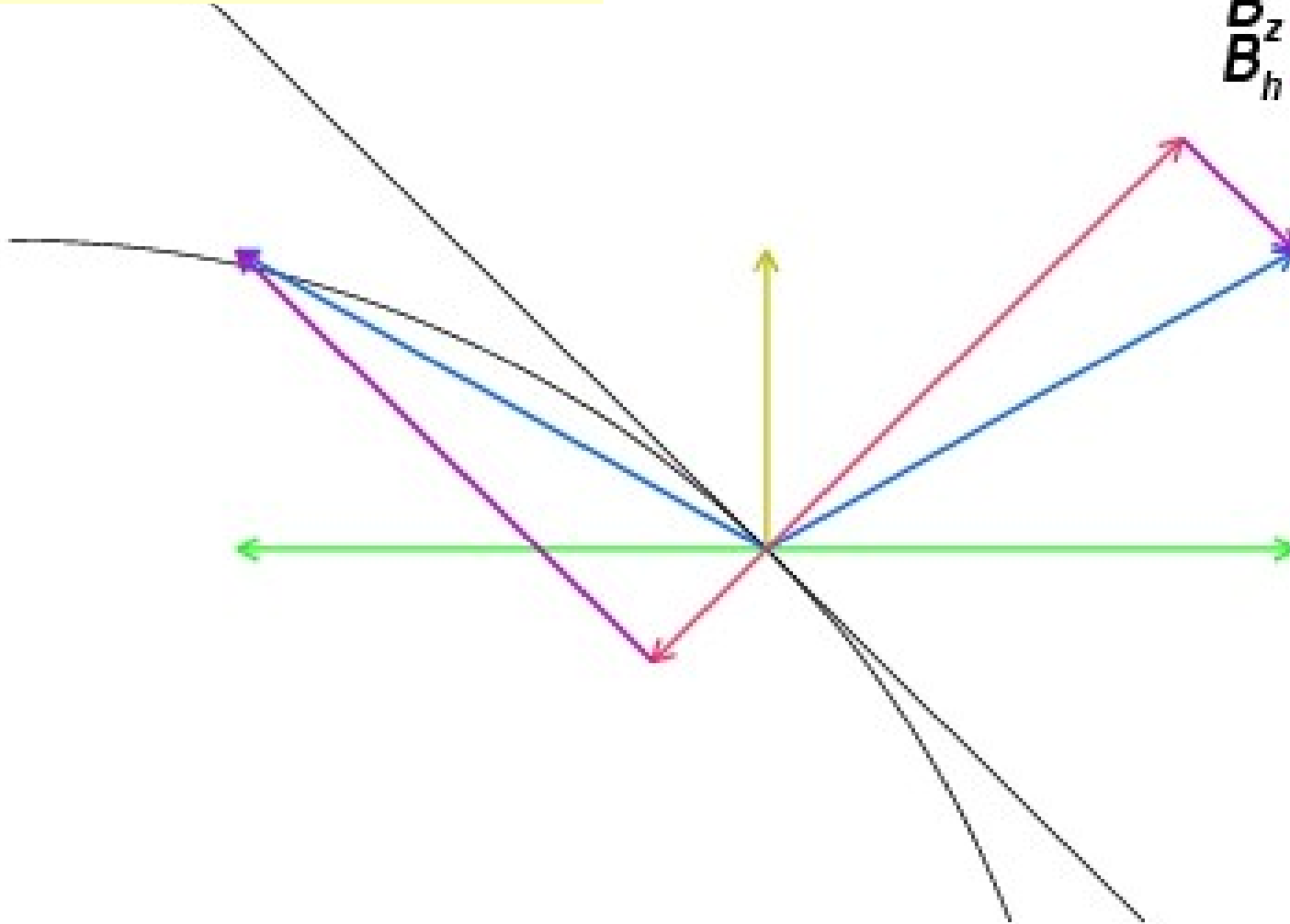
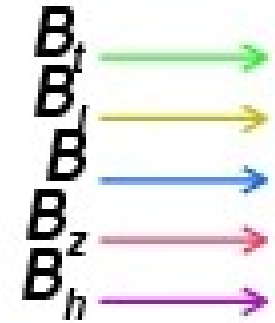


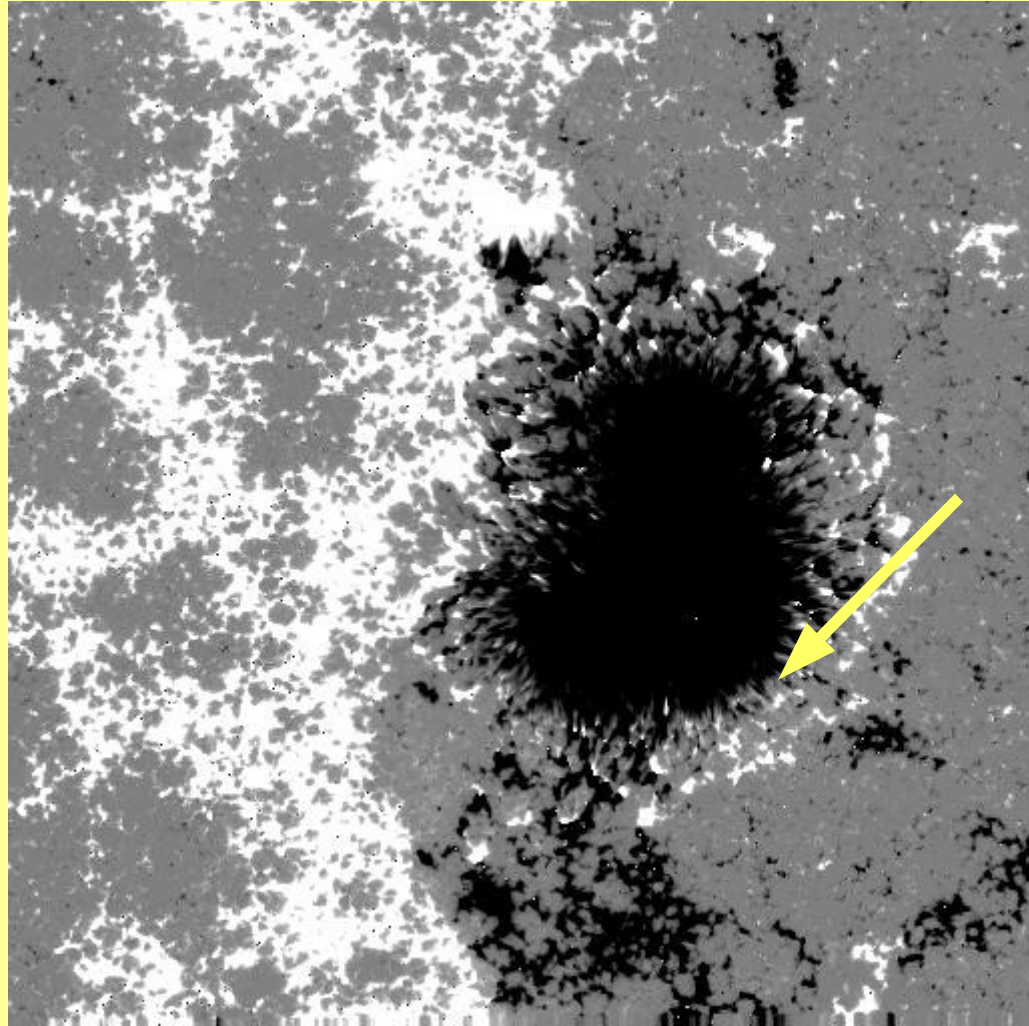
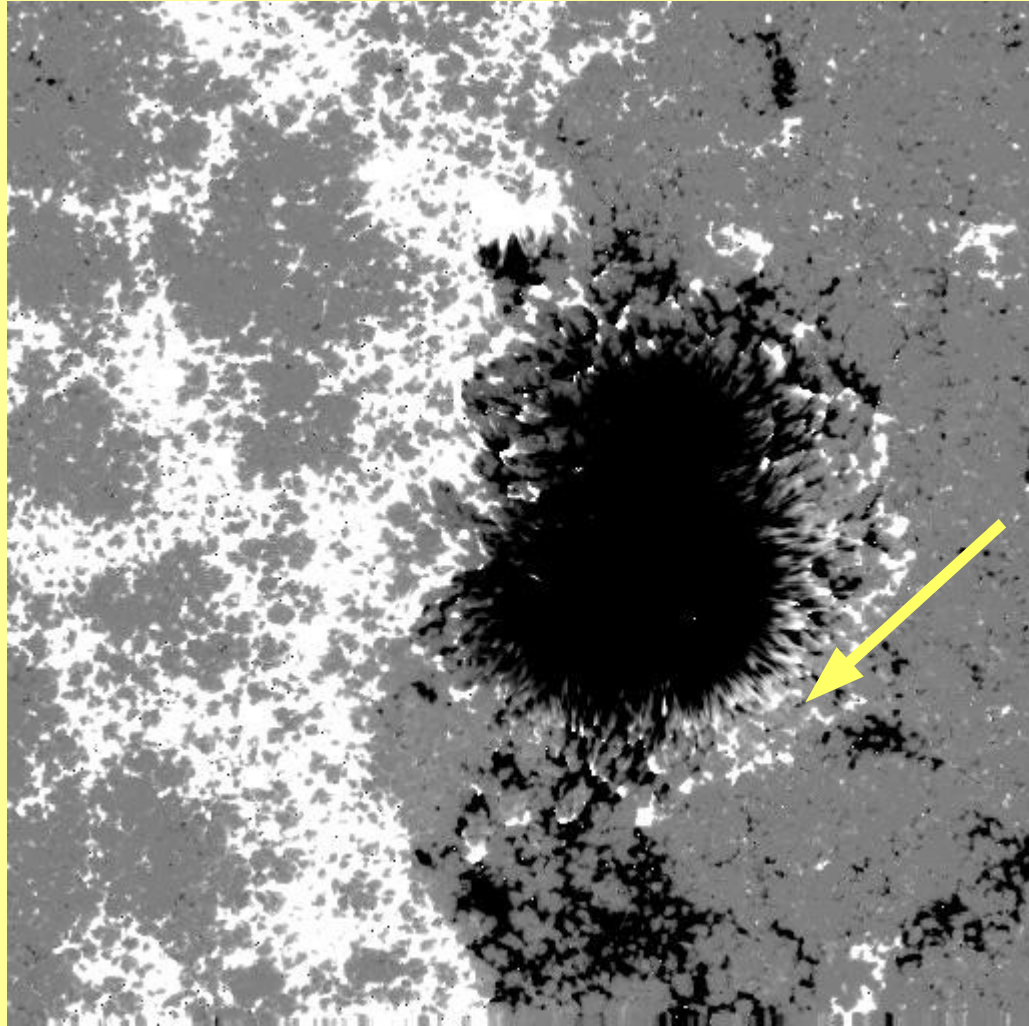
B_{trans} direction is chosen



B_t is ambiguous; direction choice influences B , and radial component B_z , true magnetic neutral (“inversion”) line, *etc.*

 *Line of sight*





Far left: B_{\parallel} of “Japan sunspot” at S10 W11 ($\mu=0.98$) from the Hinode SP; some false positive penumbral areas due to projection.

Right: B_z , radial field. Even at $\mu=0.98$, $\sum B_{\parallel} \neq \sum B_z$

Ambiguity resolution:

- ***All methods follow same two steps:***

- Assume a model field
- Choose azimuth which best matches the model field: $\mathbf{B}_t^{model} \cdot \mathbf{B}_t^{obs} > 0$

- ***Differences come in model chosen,....***

- Potential field, non-potential field, zebra-stripes...
 - There are different ways to compute a potential field....
- Same at all scales? Or a different model for large- and small-scale structures?
- Most consistent with ____ ($\nabla \cdot \mathbf{B} = 0$? $J_z = 0$? Multi-fractal? Smoothness?)

- ***... and how to implement “best match”.***

- Manually evaluate (“by my eye”)
- Iteratively pixel-by-pixel with (or without) neighboring pixel results?
- Optimize a global function
- Down-hill gradient, Multi-dimensional conjugate gradient,
- Genetic, Amoeba, others....

NWRA's Automated Ambiguity Resolution for HMI: General approach

- **Loosely based on the “Minimum-Energy Approach”:**

- Minimize the functional
$$E = \sum \left(\lambda |J_z| + \nabla \cdot \vec{B} \right)$$

- **J_z requires derivatives in the horizontal, heliographic plane**

- J_z employed rather than some approximation to J , to increase speed and reduce need for additional derivatives.

- **$\nabla \cdot \mathbf{B}$ requires derivatives in the *vertical* as well as horizontal direction.**

- The derivatives for $\partial B_z / \partial z$ are computed from a potential field using the observed unambiguous line-of-sight field as the boundary.
 - Tests showed derivatives from the potential field were adequate if combined with a robust optimization

NWRA's Automated Ambiguity Resolution, cont'd.

- **Global Optimization: Simulated Annealing is used to minimize the functional in strong-field areas.**
 - **Cooling schedule can be modified to best suit pipeline or targeted science.**
- **Weak-field areas solved by acute-angle to nearest-neighbor.**
 - **Propagate “correct” solution to areas dominated by noise.**

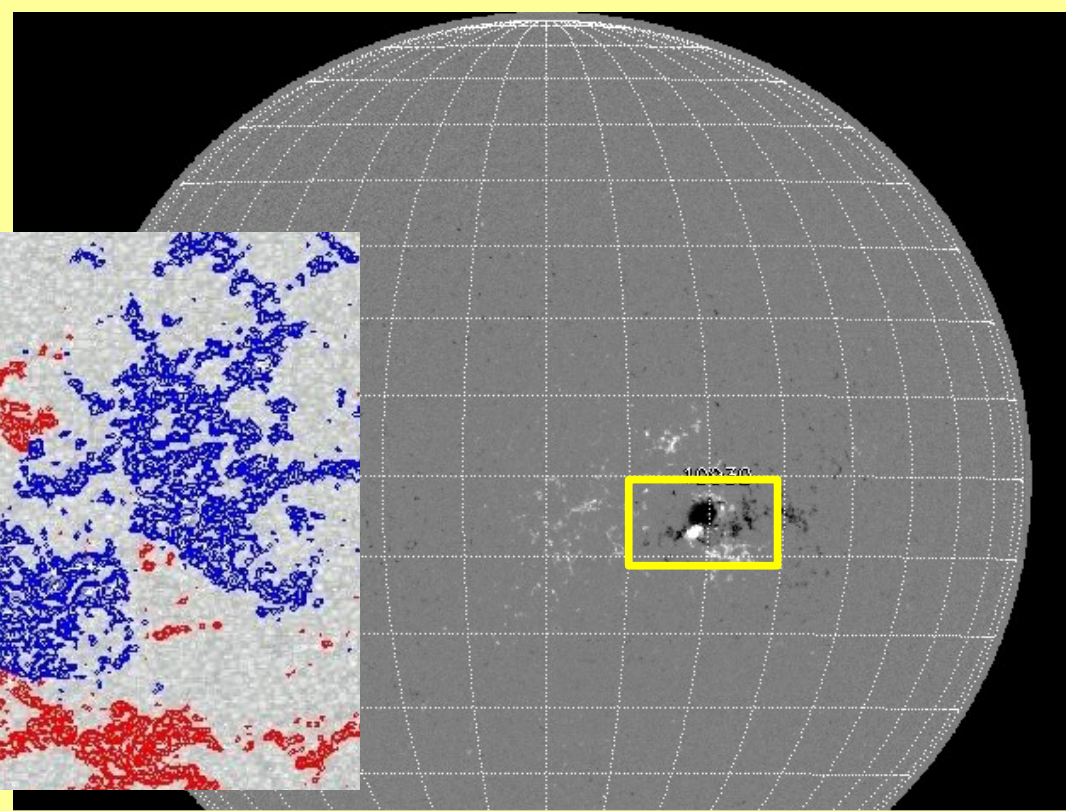
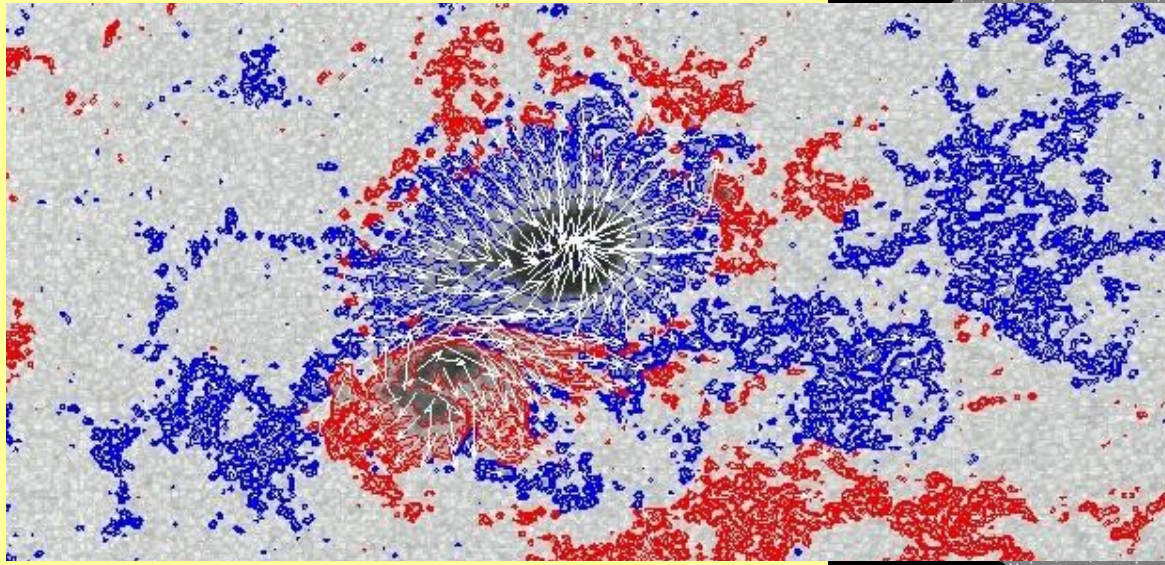
Why “Minimum Energy” approach?

- **Best-Performing automated algorithm when tested against a variety of modeled observational challenges:**

- **highly-mixed potential/non-potential,**
- **off-disk-center constant twist**
- **off-disk-center constant twist with added photon noise**
- **limited spatial resolution**

See Metcalf et al 2006;
Leka et al 2009 (in press)

Details: Magnetic Concentrations ("the Patches"): IN PIPELINE



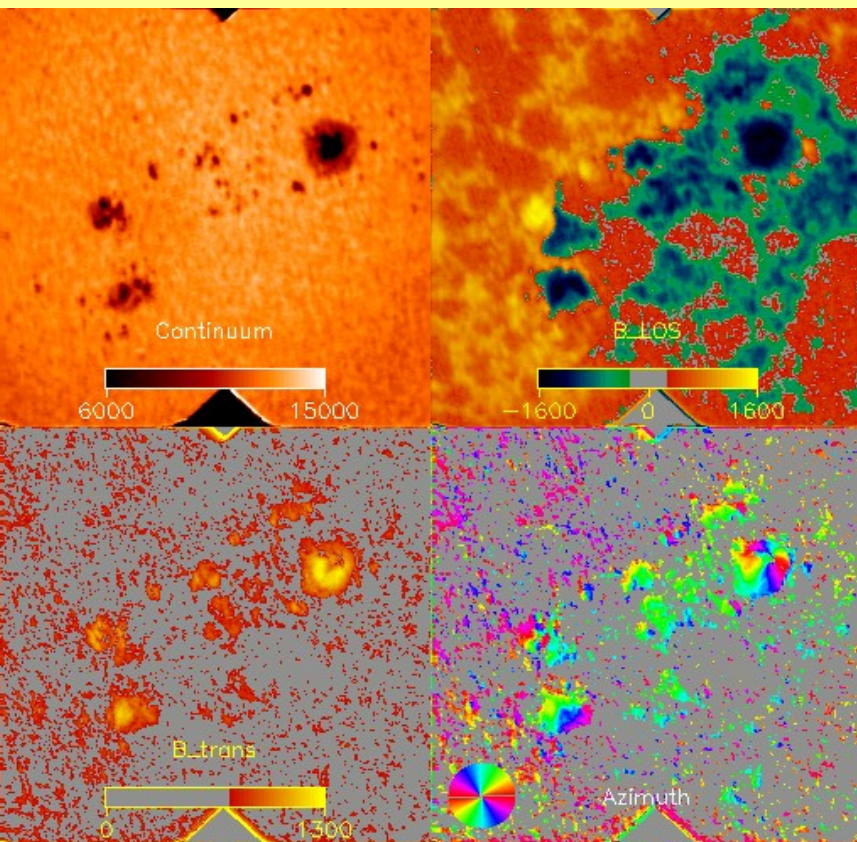
- Planar approximation: patch is approximated as a plane with a tangent point at the center.
 - can use FFTs for speed.
- Quick-Look:
 - Fast annealing schedule, higher threshold for annealing
 - Options are built-in for potential-field acute-angle and nearest-neighbor smoothing, as needed for speed.
- Science-Grade:
 - slower schedule, lower thresholds (anneal every pixel if possible)

Test data:

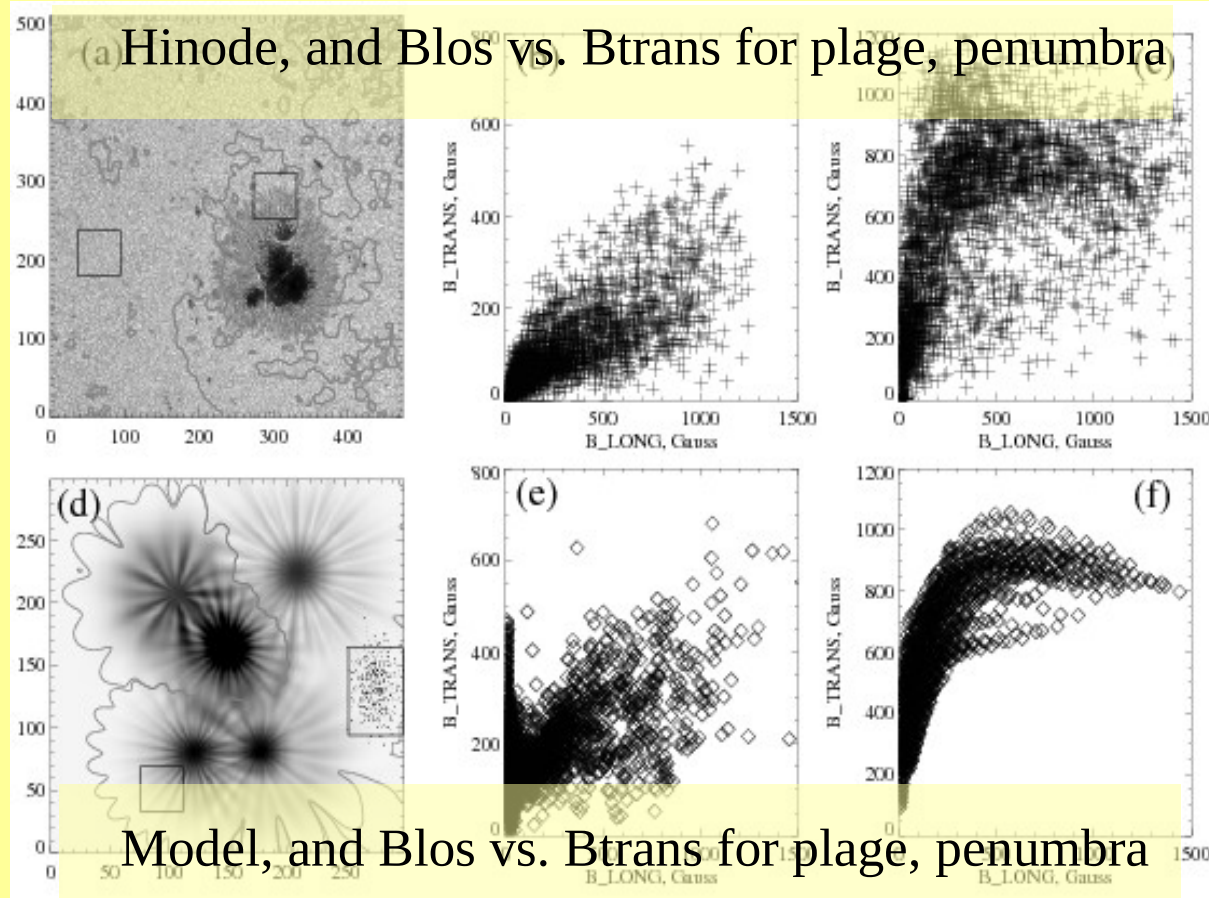
Synthetic: test algorithm against noise, spatial resolution

Hinode: high-resolution, various noise effects

Imaging Vector Magnetograph: instrument design very similar to HMI



AR9767_20020104.1752



Model, and Blos vs. Btrans for plage, penumbra

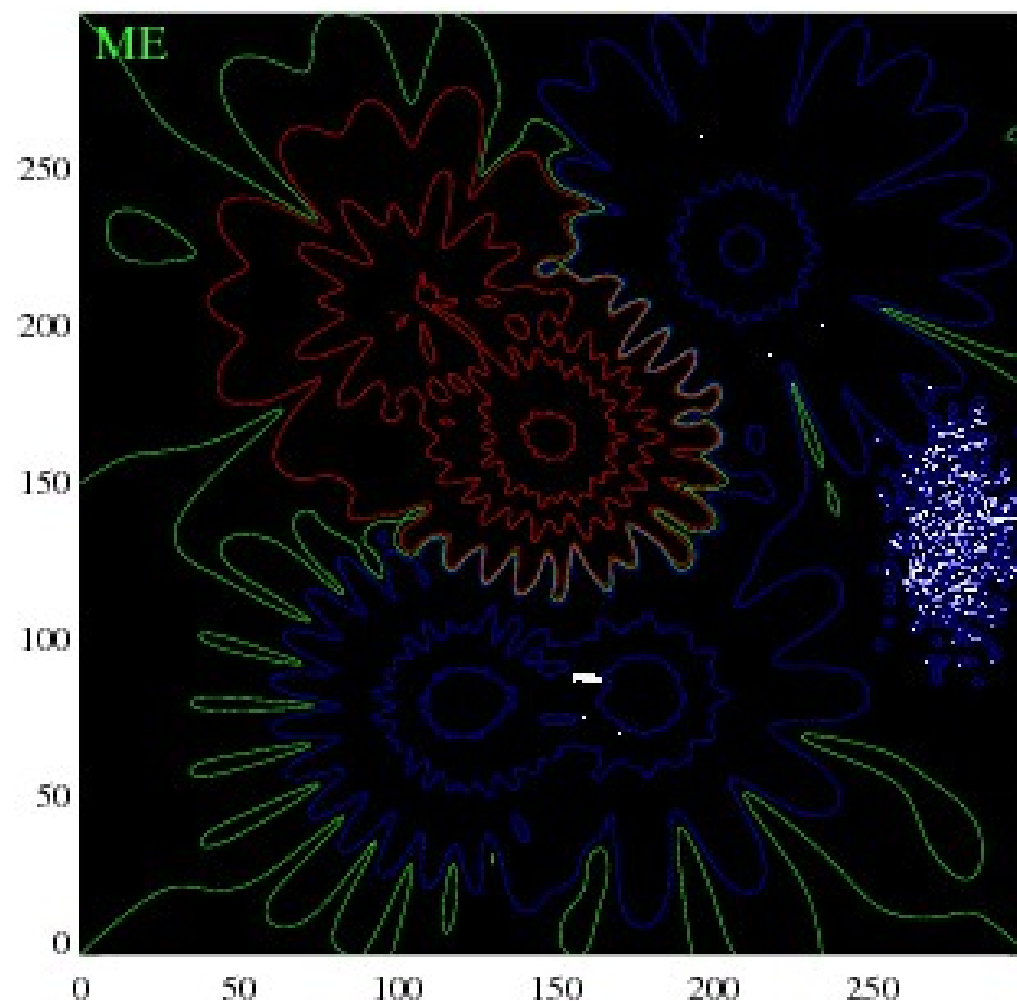
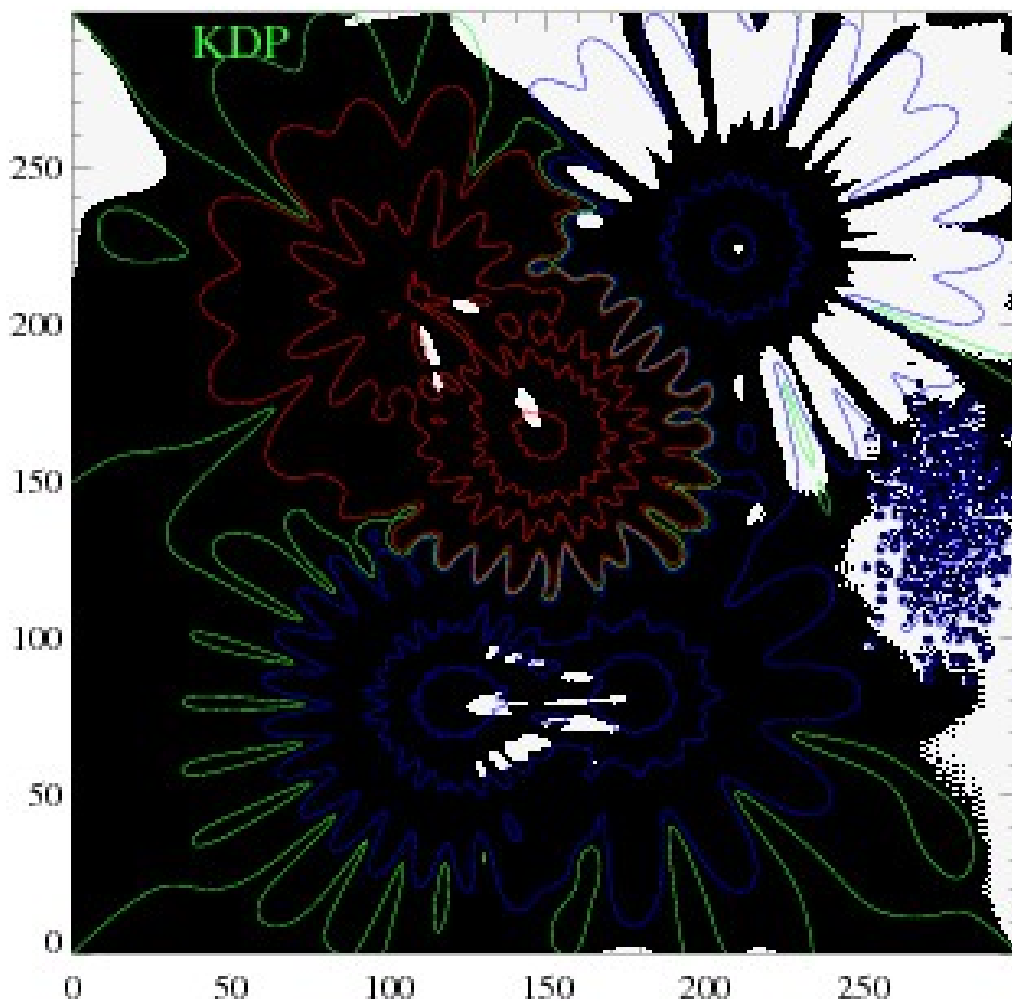
IVM data, 2002:

Continuum, Blos,
Btrans, Bazimuth

Model Data: bin10, or 0.3'' resolution, black=correct, white=incorrect:

Potential-Field Solution

NWRA Minimum-Energy Solution



M_{area}

M_{Bt}

M_{Jz}

$M_{\text{delta-B}}$

0.83

0.98

-1.11

74.0G

1.00

1.00

0.80

0.8G

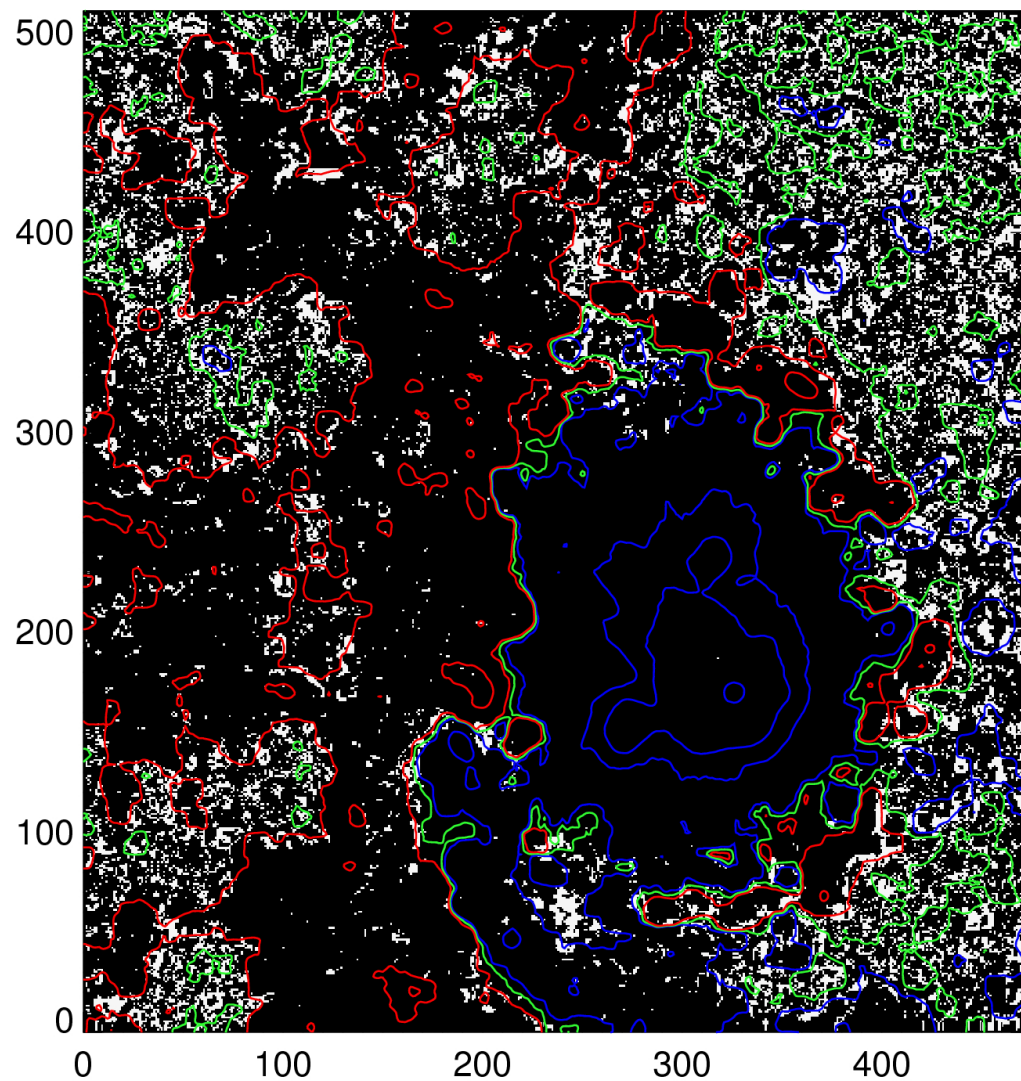
Hinode/SP example:

AR 10953 30 April 2007
during filament formation
(same as earlier slide) .

White/Black: where ME0,
AZAM dis/agree.

Result: Good agreement in
spot, filament-formation area,
and most of the plage regions.

Very weak-signal areas, well,
garbage in, garbage out....



	M_{area}	M_{flux}	M_{Bt}
<i>Minimum-Energy Solution vs AZAM</i>	0.86	0.98	1.00

- *No time-series continuity algorithm* (that is research, not pipeline code.)

Details: Full-Disk Vector Magnetograms

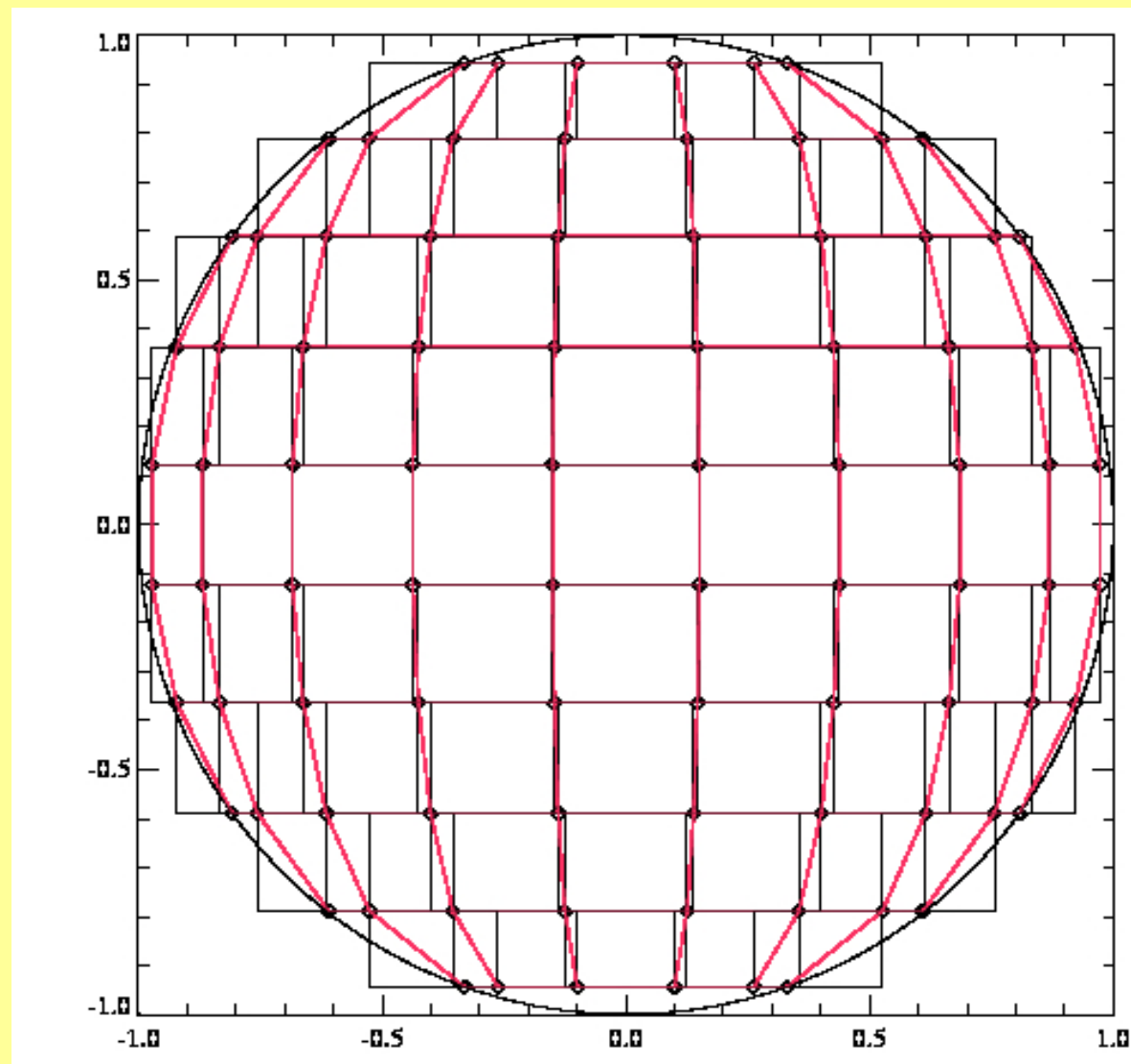
Status: In progress.

Facts of Life:

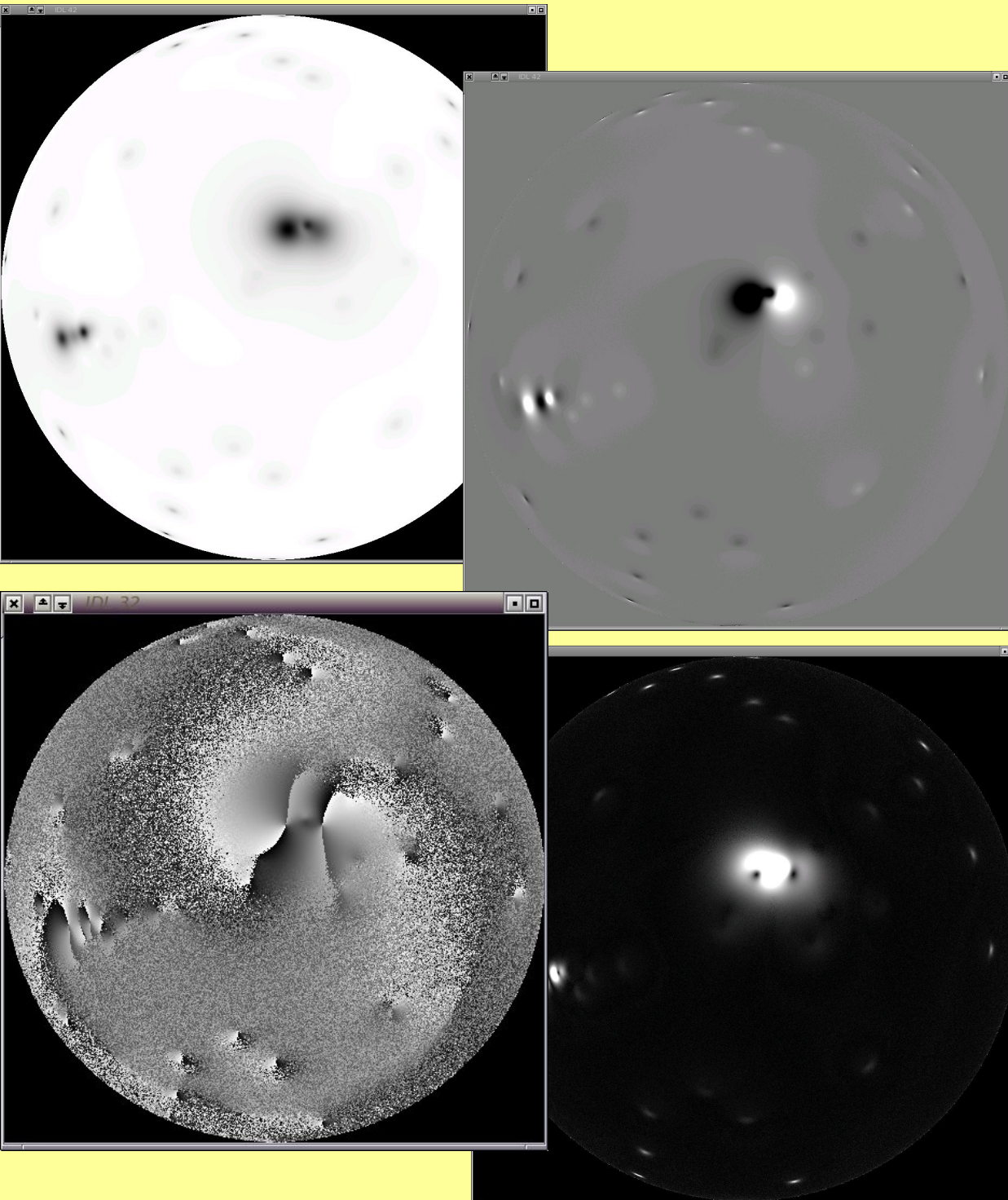
- **Curvature now important:**
 - FFTs can no longer be used,
 - Algorithms get very slow
- **Lots of pixels:**
 - Speed is crucial, however
 - any approach which employs tiling *must not result in discontinuities* in final product

Approach

- **The required derivatives** are calculated using Mollweide-projection tiles and planar approximation (speed)
- **Annealing** occurs over full disk
 - utilize strong-field masking if available.



Details: Full-Disk Vector Magnetograms, cont'd: Full-Disk test data.



- Multiple point-source collections on a sphere.
- Each “active region” has a different force-free twist parameter α ; resulting entire configuration is thus not force-free.
- There is effectively a preferential polarity in the two hemispheres (results in a net dipole moment).
- Magnetogram “sampled” at $\approx 2''$.
- Stokes polarization spectra were calculated at each pixel based on Milne-Eddington stationary atmosphere
- Photon-noise added at $\sigma I/I_c \approx 10^{-3}$
- Re-inverted assuming same restrictions.

RESULTS:

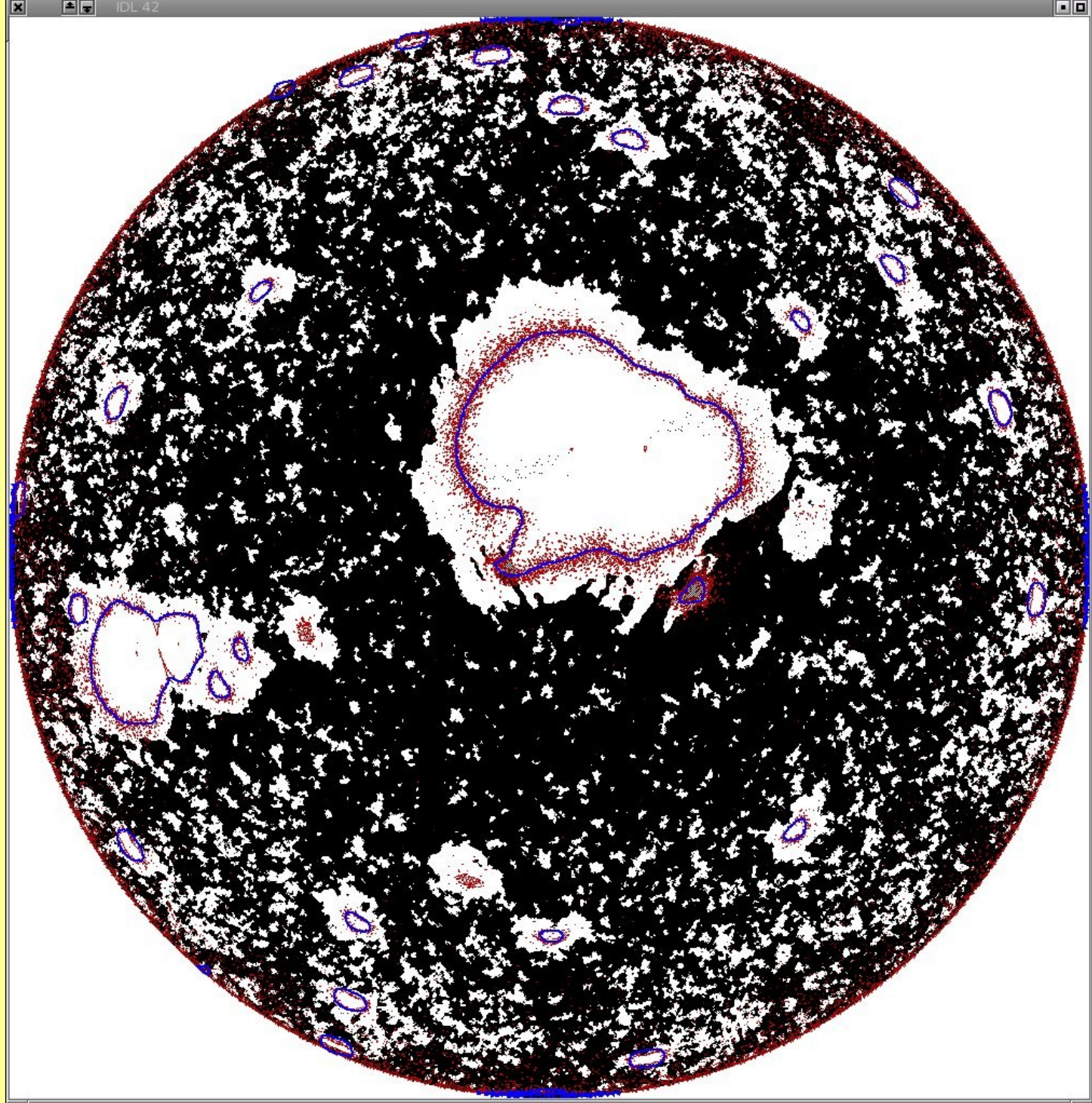
White: where correct for all of 10 different random-number seeds.

Red: contour of the threshold used for smoothing:

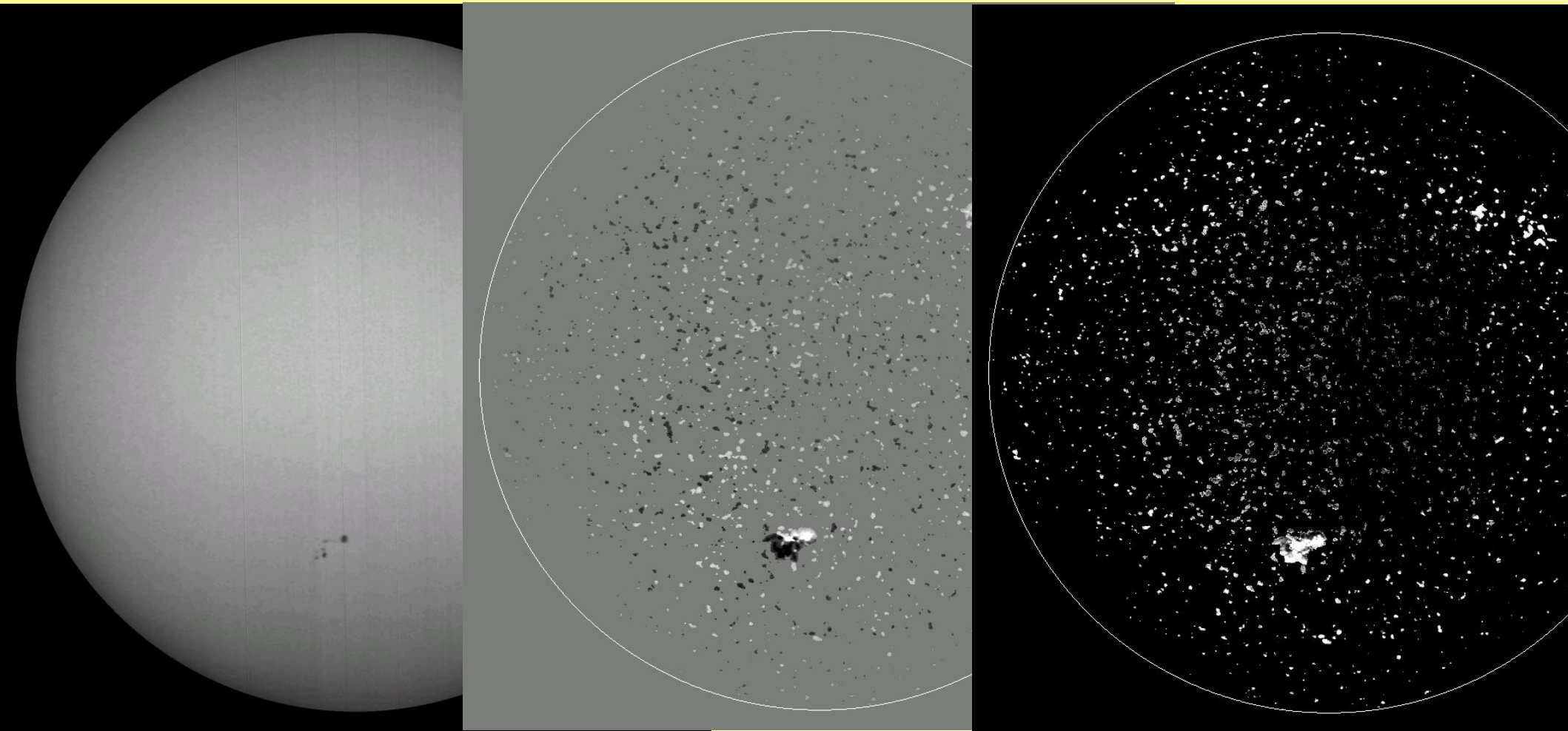
$B_{\text{trans}}=100G$.

Blue: smoothed 100G contour.

Interpretation: correctly-resolved areas generally extend beyond threshold boundaries. No tiling boundaries visible.



A recent attempt to apply method to SOLIS data:

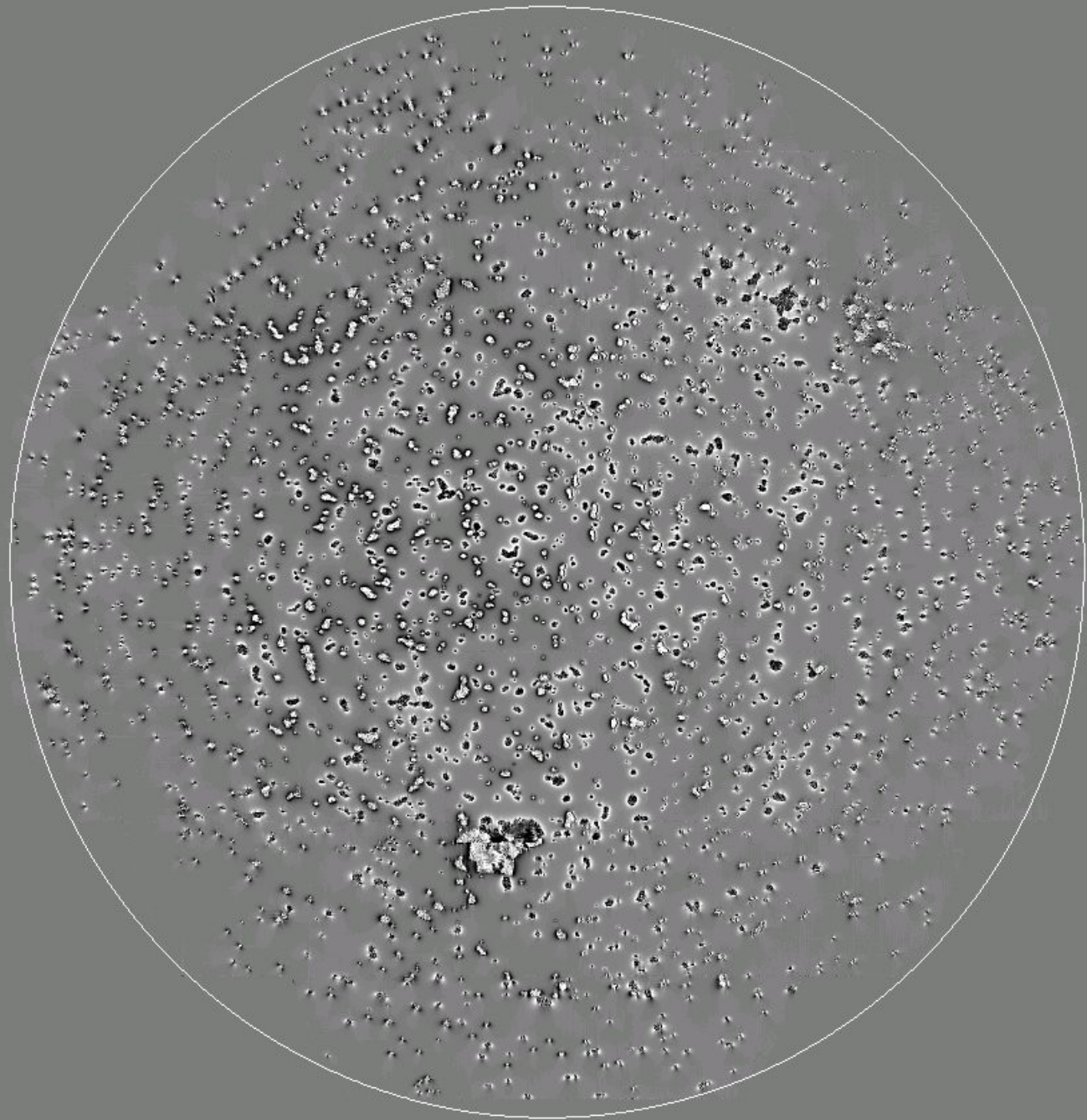


Full-disk scan 2009 July 04 15:12 UT. Fully-inverted w/ Milne-Eddington. SOLIS ME data are inverted only above a set polarization threshold.

Problem:

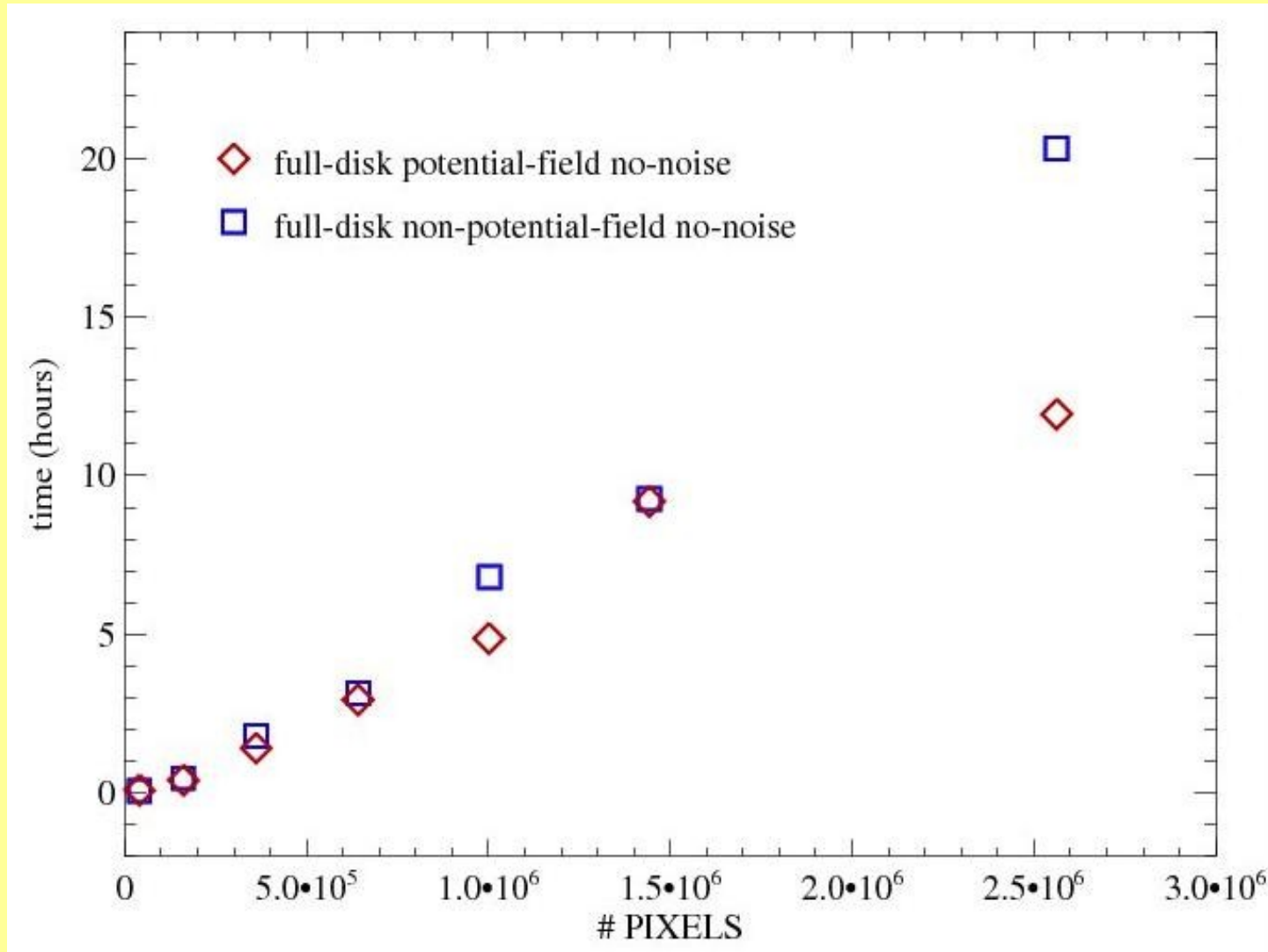
Computed derivatives (required for $\nabla \cdot \mathbf{B} = 0$) suffer serious ringing due to abrupt transition between inverted and non-inverted data (“cliffs”). Ambiguity resolution with the minimum-energy method using these derivatives...wasn't good.

HMI will invert every pixel and this should not be a problem.



Speed:

Test different resolutions of model full-disk data using one core of a quad-core 2.6GHz linux machine (similar to n02 here).



(This is why we (1) need more processors and (2) are working on implementing strong-field masking for annealing, so that we're not spending time annealing data which is just noise.)

Summary

- Ambiguity resolution a *necessary evil* for vector magnetic field data
- Method and code based on a well-tested algorithm will be in the HMI pipeline, with options built-in to suit both quick-look and science-grade data.
- Things to consider:
 - Surface potential field is being calculated during this step. For efficiency, should these products be saved?
 - There is presently no explicit handling of time-series data. This may be incorporated later after research projects are finished.
 - Uncertainties in magnetic-field data products may be a mix of propagation of errors from photometry, χ^2 from fitting/inversion, and probabilistic uncertainties from ambiguity resolution. How can we quote a single uncertainty? *Should* we quote a single uncertainty?

Just a few different approaches:

● **Potential-field acute-angle**

- Using *FFTs* (K. Leka, J. Jing) with/without flux balance, boundary padding
- Based on *Green's Function solution* (J. Li, V. Yurchyshyn)

● **Large-Scale Potential method** (A. Pevtsov)

- assumes large-scale fields are potential, deviations increase with spatial resolution

● **Linear Force-Free Acute-Angle method** (H.N. Wang)

- Best-fit to LFFF field consistent with coronal-loop observations

● **Uniform Shear Method** (Y.J. Moon)

- assumes shear angle follows a normal distribution

● **Magnetic Pressure Gradient** (J. Li)

- assumes magnetic pressure decreases with height

● **Minimum Structure** (M. Georgoulis)

- Minimize a component of current analytically, then numerical smoothing

● **NonPotential Magnetic Field Calculation** (M. Georgoulis)

- Finds the distribution of B_z whose potential extrapolation plus a calculated non-potential component best matches the observed heliographic field.

● **Pseudo-Current Method** (A. Gary)

- Minimizes J_z^2 by locating sources of non-potentiality

● **U. Hawai`i Iterative Method (Metcalf, Fan & Leka)**

- Iterates locally to minimize J_z and $\text{div}(\mathbf{B})$, then acute-angle neighbor smooths

● **Minimum-Energy solution (Metcalf)**

- Global optimization of J and $\text{div}(\mathbf{B})$, numerous weighting options

- **Early synoptic vector magnetic field instruments made it *very* clear *very* early on that *automated* data-reduction algorithms were required, *including ambiguity resolution*.**

- U.Hawai`i's Haleakala Stokes Polarimeter,
- Imaging Vector Magnetograph;
- NAOJ/Mitaka's Flare Telescope,
- MSFC's vector magnetograph, BBSO's video magnetograph.
- Observer-driven instruments: less data and less automation needed. Human-based interactive approaches were possible.

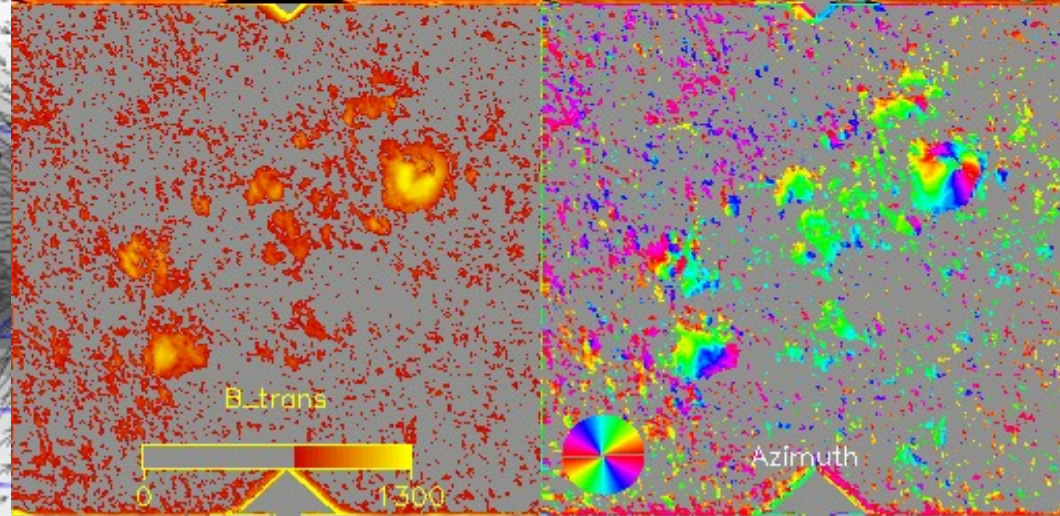
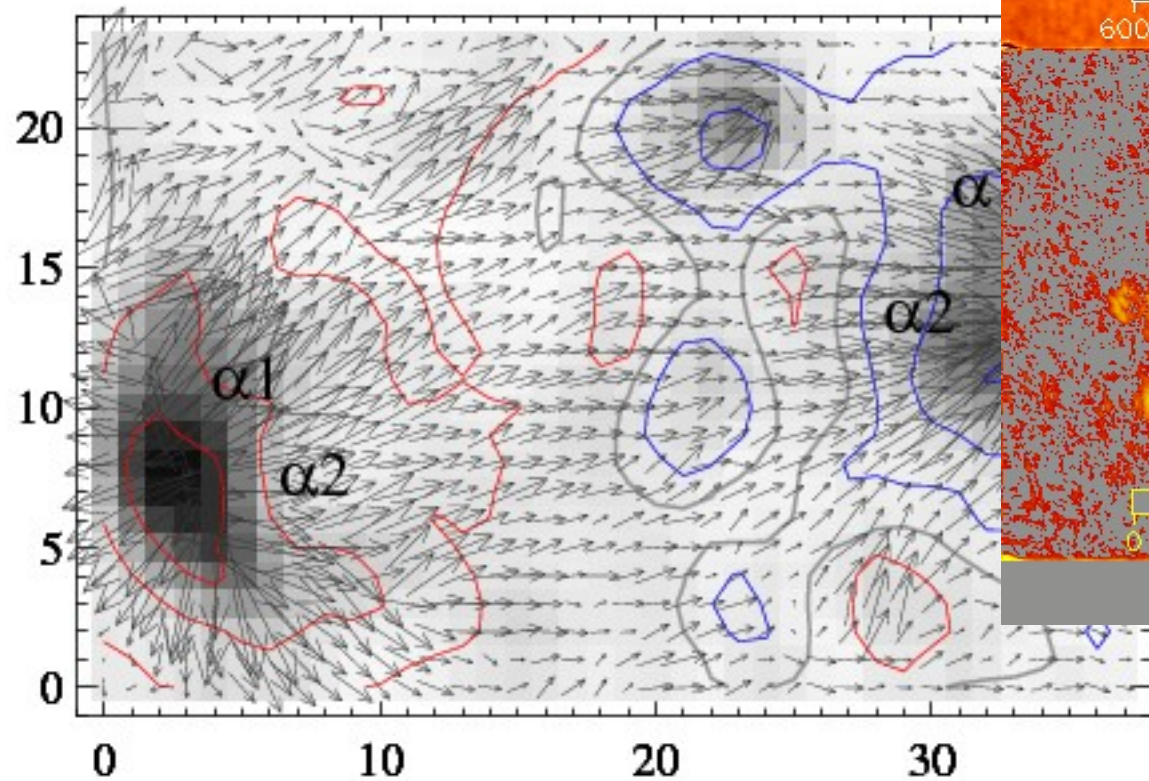
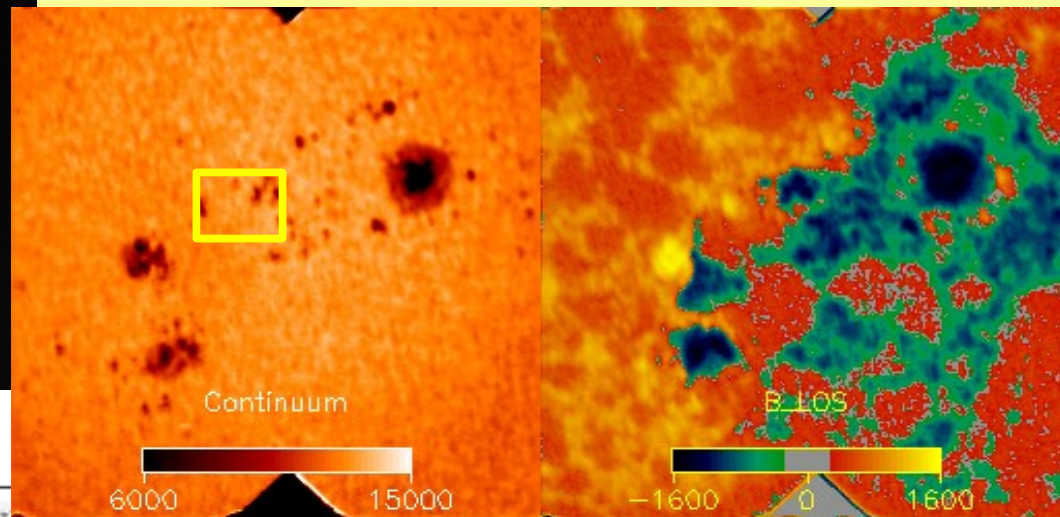
- **With high-resolution and high-cadence data (Hinode, ATST, SDO/HMI, SOLIS), algorithm(s) are required with high *performance value* (courtesy C. Henney):**

- *Accurate enough for science goals*
- Stable for conditions of interest (e.g. Full-disk)
- Fast relative to inversion time,
(define $\text{Time} = \text{InversionTime} / \text{AmbigTime}$)
- Is the algorithm automatic?
If yes, (set $\text{Auto} = 1$, otherwise $\text{Auto} = \infty$)

- **$\text{Merit} = (\% \text{ accuracy} * \text{Stability} + \text{Time}) / \text{Auto}$**

Continuing Challenges:

- Visualization



AR9767_20020104.1752